Observation of Enhanced Raman Scattering for Molecules Adsorbed on TiO2 Nanoparticles: Charge-Transfer Contribution

ARTICLE *in* THE JOURNAL OF PHYSICAL CHEMISTRY C · DECEMBER 2008

Impact Factor: 4.77 · DOI: 10.1021/jp8074145

6 AUTHORS, INCLUDING:

Weidong Ruan
Jilin University
52 PUBLICATIONS **878** CITATIONS

SEE PROFILE

Bing Zhao
Jilin University
276 PUBLICATIONS **5,020** CITATIONS

SEE PROFILE

Article

Observation of Enhanced Raman Scattering for Molecules Adsorbed on TiO Nanoparticles: Charge-Transfer Contribution

Libin Yang, Xin Jiang, Weidong Ruan, Bing Zhao, Weiqing Xu, and John R. Lombardi

J. Phys. Chem. C, **2008**, 112 (50), 20095-20098 • Publication Date (Web): 18 November 2008

Observation of Enhanced Raman Scattering for Molecules Adsorbed on TiO_2 Nanoparticles: Charge-Transfer Contribution

Libin Yang,[†,‡] Xin Jiang,[‡] Weidong Ruan,[†] Bing Zhao,*[,†] Weiqing Xu,[†] and John R. Lombardi*[,§]

State Key Laboratory of Supramolecular Structure and Materials, Jilin University, Changchun 130012, People's Republic of China, College of Chemistry and Pharmacology, Jiamusi University, Jiamusi 154007, People's Republic of China, and Department of Chemistry, The City College of New York, New York 10031

Received: August 18, 2008; Revised Manuscript Received: October 16, 2008

Surface-enhanced Raman scattering from molecules adsorbed on TiO_2 nanoparticles has been observed. This is attributed to the dominant contribution of the TiO_2-to-molecule charge-transfer mechanism. The charge-transfer process is largely dependent on the intrinsic nature of the adsorbed molecules and the surface properties of the semiconductor. Both the stronger electron attracting ability of groups *para*- to the mercapto group bonded with TiO_2 surface and the plentiful surface states of TiO_2 nanoparticles are favorable to TiO_2-to-molecule charge-transfer and SERS for molecules adsorbed on TiO_2.

Introduction

Surface-enhanced Raman scattering (SERS) has attracted considerable attention in various fields, such as electrochemistry, surface science, catalysis, and chemical and biomolecular sensing, due to its broad applied prospects. Recent advances in SERS spectroscopy have made single-molecule detection possible,[1−3] single-molecule SERS is estimated to display an enhancement factor of $10^{12}-10^{15}$. At present, SERS active substrates have been restricted to the noble metals (Ag, Au, Cu) and transition metals (Pt, Pd, Ru, Rh, Fe, Co and Ni).[4−8] Only a few studies with SERS on nonmetallic surfaces have been reported. Quagliano[9] has detected Raman signals from pyridine molecules adsorbed on InAs/GaAs surfaces. Yamamoto[10] has reported some evidence for SERS on small GaP particles. Wang Yanfei et al.[11] observed 10^2 enhancement from 4-mercaptopyridine adsorbed on CuO nanocrystals. A lack of SERS substrate limits the breadth of practical applications for SERS in various materials, especially in semiconductor materials widely used in electrochemistry, catalysis and other industries. The source of the enhancement mechanism of semiconductor-based SERS substrates is still under active investigation.

Herein, we investigate Raman scattering of molecules adsorbed on TiO_2 nanoparticles. The present study is of interest from two points of view. First, we observe the SERS phenomenon on TiO_2 nanoparticles. This research not only extends the applicability of Raman spectroscopy, as a SERS technology to investigate the adsorption problems on semiconductor surfaces, but also develops a novel semiconductor SERS substrate. Second, a possible SERS mechanism on TiO_2 is proposed, which may be helpful to understand the SERS mechanism related to semiconductor materials as well as to understand the charge transfer action between adsorbates and semiconductor materials.

* Corresponding authors. Fax: +86-431-85193421 (B.Z.). E-mail: zhaob@mail.jlu.edu.cn (B.Z.); lombardi@sci.ccny.cuny.edu (J.R.L.).
[†] Jilin University.
[‡] Jiamusi University.
[§] The City College of New York.

Experimental Section

Chemicals. 4-Mercaptobenzoic acid (4-MBA), 4-mercaptopyridine (4-MPY), and 4-aminothiophenol (PATP) were purchased from Acros Organics Chemical Co. and used without further purification. The other chemicals were all analytical grade without further purification too. Purified water produced by Hangzhou Wahaha Group Co. was used in all experiments.

Sample Preparation. TiO_2 nanoparticles were prepared by a sol-hydrothermal process.[12] First, a mixed solution of 5 mL of tetrabutyl titanate and 5 mL of anhydrous ethanol was added dropwise into another mixed solution, consisting of 20 mL of anhydrous ethanol, 5 mL of water and 1 mL of 70% nitric acid, at room temperature under roughly stirring to carry out hydrolysis. Subsequently, the yellowish transparent sol was obtained by continuously stirring for 1 h. The as-prepared sol was kept at 160 °C for 6 h in a stainless-steel vessel, then cooled to room temperature. The sol-hydrothermal production was dried at 60 °C for 24 h. Finally, TiO_2 nanoparticles were obtained by calcining the TiO_2 sol-hydrothermal production at certain temperature (450−550 °C) for 2 h.

TiO_2 nanocrystals surface-modified by molecules were obtained as follows: 20 mg of TiO_2 nanocrystals were dissolved in 10 mL of 4-MBA, 4-MPY, or PATP (1×10^{-3} M) ethanol solution, and the mixture was stirred for 2 h. Then, the precipitate was centrifuged and rinsed with purified water once more. TiO_2 nanocrystals modified by 4-MBA, 4-MPY, or PATP were obtained.

Sample Characterization. The crystal structure of TiO_2 sample was determined by X-ray diffraction using a Siemens D5005 X-ray powder diffractometer with a Cu Kα radiation source at 40 kV and 30 mA. The surface morphology of the sample was measured on a JEOL JSM-6700F field emission scanning electron microscope (FE-SEM) operated at 3.0 kV. The electronic absorption spectra were recorded on a Shimadzu UV-3600 UV−vis spectrophotometer. Raman spectra were obtained with a Renishaw Raman system Model 1000 spectrometer. The 514.5 nm radiation from a 20 mW air-cooled argon ion laser was used as exciting source. Data acquisition was the result of three 30s accumulations for all molecules

10.1021/jp8074145 CCC: $40.75
Published on Web 11/18/2008

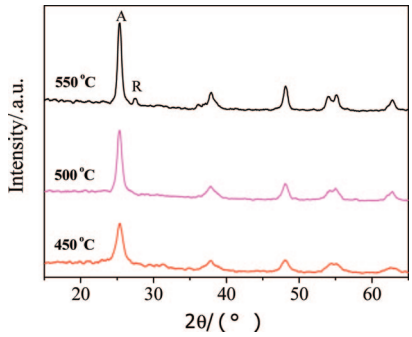

Figure 1. XRD patterns of TiO_2 nanoparticles calcined at different temperature.

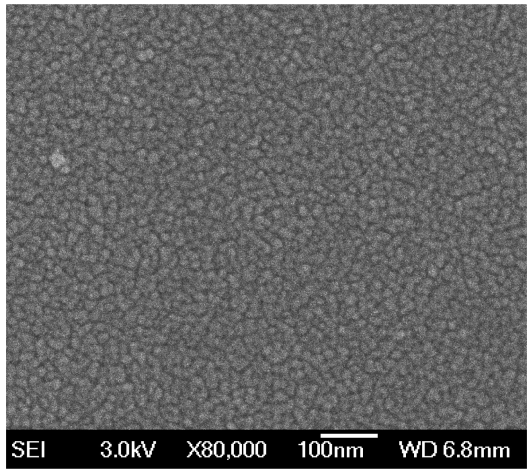

Figure 2. SEM image of TiO_2 nanoparticles calcined at 450 °C.

adsorbed on TiO_2 nanoparticles. The resolution of the Raman instrument was ca. 4 cm^{-1}.

Results and Discussion

Measurements of XRD and SEM. Figure 1 shows the XRD patterns of TiO_2 nanoparticles calcined at different temperature. In general, the XRD peaks at $2\theta = 25.3°$ and $2\theta = 27.4°$ are identified as the characteristic diffraction peaks of the anatase and rutile crystal phase of TiO_2, respectively.[13] Figure 1 reveals that TiO_2 nanocrystals calcined at 450 and 500 °C were pure anatase phase TiO_2, when increasing the calcination temperature to 550 °C, there was a small amount of rutile phase appearing. It can be observed that the diffraction peaks increase in intensity and narrow in width with the calcination temperature rising from 450 to 550 °C, indicating that the degree of crystallinity of samples increases and the crystalline size also increases. The crystallite sizes D were about 8.6, 10.9, and 12.8 nm, respectively. These values were estimated from the half-bandwidth of the corresponding X-ray spectral peak by the Scherrer formula:[13,14] $D = k\lambda/(\beta \cos \theta)$. The SEM image is shown in Figure 2. The samples are spherical, with a narrow size distribution.

Measurements of UV−Vis DRS. UV−vis spectra were carried out to investigate the effect of adsorbed molecules on optical properties of TiO_2 nanocrystals. Figure 3 shows the UV−vis DRS spectra of pure and surface-modified TiO_2 nanoparticles calcined at 450 °C. All samples exhibited a wide optical absorption in the range below 400 nm, which resulted from band-band transition of the TiO_2 nanocrystals according to its band energy 3.2 eV. It can be seen in the figure that the photoabsorption threshold of surface-modified TiO_2 occurs blue-

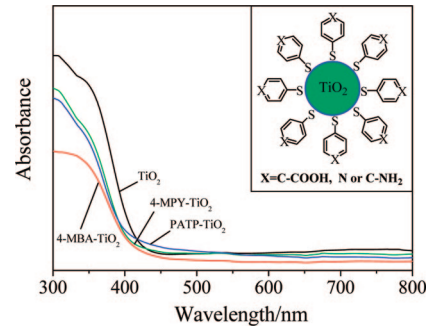

Figure 3. UV−vis DRS spectra of different samples and the sketch (inset) of 4-MBA, 4-MPY and PATP adsorbed on TiO_2 nanoparticles.

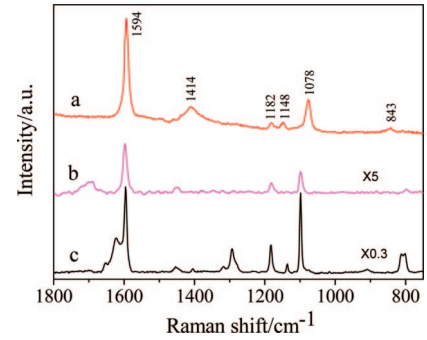

Figure 4. SERS spectrum of 4-MBA adsorbed on TiO_2 (a) and the normal Raman spectra of 4-MBA in 0.1 M ethanol solution (b) and in the solid state (c).

shifted to a different degree compared with that of unmodified TiO_2. It is especially large for 4-MBA surface-modified TiO_2. These shifts can be interpreted as the result of an appreciable interaction between the adsorbed molecules and the TiO_2 substrate, the mode of the molecules surface-modified TiO_2 nanocrystals is shown in the inset of Figure 3. Similar results were reported in ref 15 for dye molecules adsorbed on TiO_2 surfaces and ref 11 for 4-MPY surface-modified CuO nanocrystals.

SERS Spectra of 4-MBA on TiO_2. Figure 4 shows the SERS spectrum of 4-MBA adsorbed on TiO_2 nanocrystals from 10^{-3} M ethanol solution (a) and the normal Raman spectra of 4-MBA in 0.1 M ethanol solution (b) and in the solid state (c). The SERS spectrum of 4-MBA adsorbed on TiO_2 (Figure 4 a) was consistent with those previously reported for 4-MBA adsorbed onto ZnO nanocrystals[16] and dominated by the strong bands at about 1594 and 1078 cm^{-1}, which are assigned to ν_{8a} (a_1) and ν_{12} (a_1) aromatic ring characteristic vibrations, respectively. The above assignment was performed by a comparison with the spectra of 4-MBA adsorbed on Ag and Au substrates.[17] Other weak bands at about 1148 (ν_{15}, b_2) and 1182 (ν_9 a_1) cm^{-1}corresponding to the C−H deformation modes were also observed in the Raman spectrum of 4-MBA adsorbed on TiO_2 nanocrystals. It should be noticed that the SERS spectrum of 4-MBA adsorbed on TiO_2 is significantly different from the normal Raman spectra of 4-MBA ethanol solution and solid powder in both the intensity and the position of Raman peaks. It is clear that the Raman signals of 4-MBA adsorbed on TiO_2 nanocrystals are remarkably enhanced relative to 4-MBA in solution. Furthermore, the extra enhancement of the b_2 modes provides supporting evidence for the importance of charge-transfer in the enhancement mechanism.

SERS Mechanism for 4-MBA Adsorbed on TiO_2. It is now generally accepted that there are two interacting mechanisms which explain for the overall SERS effect: the electromagnetic

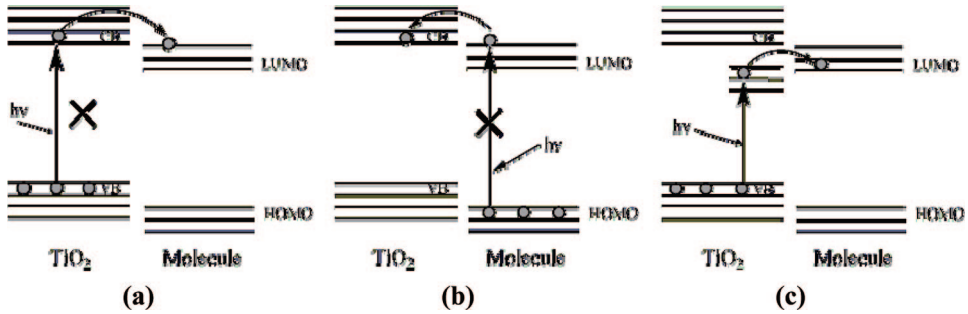

Figure 5. Modes of the charge transfer between the adsorbed molecule and TiO_2.

(EM) mechanism and the charge-transfer (CT) mechanism.[18−24] The former involves the enhancement of the optical fields at the surface and requires the incoming radiation to excite the surface plasmon resonance, resulting in a strong local enhancement of the electric field. This EM model does not require specific bonds between adsorbates and substrates and explains the enhancement at some distance from the metal surface. The latter is a resonance Raman-like process in which CT between metal and adsorbate is the intermediate stage. Direct proximity (bond) between the molecules and the substrate surface is required for the CT enhancement.

For most semiconductor materials, the surface plasmon resonant frequency is located in the infrared region, determined by the formula:,[25] $\omega_p = [4\pi ne^2/m_e\varepsilon_\infty]^{1/2}$, which is far from 514.5 nm exciting line used in our experiment. Therefore, the EM mechanism can not be the dominant contribution to the surface enhanced Raman signal for 4-MBA adsorbed on TiO_2 nanocrystals. The dominant contribution to the SERS signal in this case must be a CT mechanism. This is indicated by the observation of enhancement of nontotally symmetric b_2 modes in the spectrum. Considering the energy band structure of TiO_2 semiconductor, charge transfer between the TiO_2 nanoparticles and adsorbed molecules could possibly involve three kinds of modes as follows: (i) Electrons from the valance band (VB) of TiO_2 are excited to the conduction band (CB) by the incident light with the energy no less than TiO_2 band gap energy (3.2ev) and then injected into the LUMO of the adsorbed molecules (Figure 5a). (ii) Electrons from the HOMO of the adsorbed molecules are excited to the LUMO by the incident light and then injected into TiO_2 CB (Figure 5b). (iii) Electrons of TiO_2 VB are excited to surface state energy levels by the incident light with the sub-band gap energy and then injected into the LUMO of the adsorbed molecules (Figure 5c). TiO_2 is a typical n-type semiconductor, and in nanoparticles, there are plenty of surface defects (i.e., surface oxygen vacancy defects), which can bind electrons and form the so-called surface state energy levels. In TiO_2 they have been located at a position 0.5 eV lower than TiO_2 CB edge.[26−29] Cao[29] et al. have experimentally verified the electronic transition related to the surface state of TiO_2 at about 400−700 nm by means of the photocurrent spectrum. In our experiment, the 514.5 nm (ca. 2.4 eV) laser used as exciting source is not sufficient to excite the electrons transitions from TiO_2 VB to CB or from the adsorbed molecules HOMO to LUMO. However, it is adequate to excite the electrons transitions from TiO_2 VB to the low-lying surface states as shown in Figure 5c. Therefore, the first two types of CT modes are ruled out, It is reasonable that the third CT mode dominantly contributes to the SERS for 4-MBA adsorbed on TiO_2 nanoparticles.

To further verify that the dominant contribution to the enhancement is TiO_2-to-molecule charge-transfer in the present

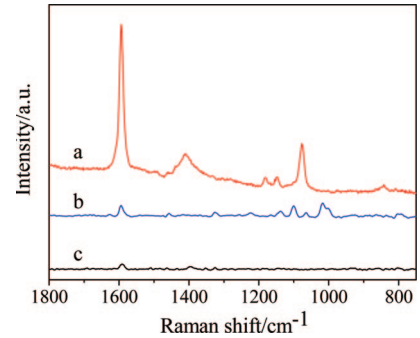

Figure 6. SERS spectra of 4-MBA (a), 4-MPY (b), and PATP (c) adsorbed on TiO_2 nanoparticles calcined at 450 °C.

study, the following experiments were performed. We varied groups para- to the mercapto group (−SH) on the benzene ring of the adsorbed molecules by using 4-MPY and PATP as well as 4-MBA as the probe molecules. The order of electron attracting ability of groups para- to the mercapto group on benzene ring is C−COOH > *N* > C−NH_2. Figure 6 shows SERS spectra of 4-MBA, 4-MPY and PATP adsorbed on TiO_2 nanoparticles. It can be seen that the order of enhancement for molecules on TiO_2 is 4-MBA > 4-MPY > PATP, which is in good agreement with attracting electron ability of para groups of mercapto group and is not the result from differences in Raman scattering cross section of molecules in our experiment, since Raman scattering cross sections of the three kinds of molecules are almost same. This demonstrates that SERS signals for the molecules on TiO_2 were certainly the result of the contribution of the TiO_2-to-molecule CT mechanism, since the stronger the electron attraction of groups para to the mercapto group bonded with the TiO_2 surface, the higher the capability of TiO_2-to-molecule CT and the stronger SERS signals for the molecules on TiO_2.

In addition, a crystallinity-dependent experiment was also carried out to examine whether the TiO_2-to-molecule CT was related to the surface states of TiO_2. Figure 7 shows SERS spectra of 4-MBA adsorbed on TiO_2 nanoparticles calcined at different temperature. It can be seen that the intensity of SERS signals for 4-MBA adsorbed on TiO_2 were remarkably decreased with the calcination temperature rising from 450 to 550 °C. The XRD measurements show the degree of crystallinity of TiO_2 samples becomes higher and the crystallite size becomes larger with increase in the calcination temperature, simultaneously the specific surface area and surface defect content of TiO_2 nanoparticles also decreased.[27] We found that the decrease of adsorption for 4-MBA on TiO_2, caused by the decrease of the specific surface areas of TiO_2 with the calcination temperature rising, was far less than $^1/_{10}$ by the UV−vis measurements of 4-MBA ethanol solution after adsorption. This indicates that we cannot explain so large a decrease in intensity of SERS

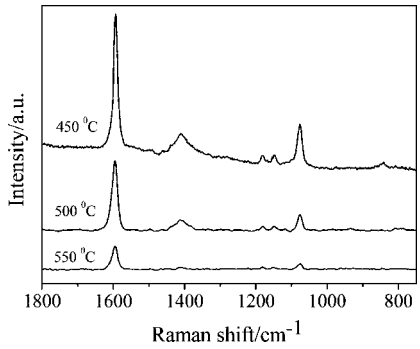

Figure 7. SERS spectra of 4-MBA adsorbed on TiO_2 nanoparticles calcined at different temperature.

signals for 4-MBA adsorbed on TiO_2 (Figure 7) with total reduction in surface area. Thus the remarkable decrease in intensity of SERS signals for 4-MBA adsorbed on TiO_2 with the calcination temperature must result from the decrease of surface defect content of TiO_2. The higher the calcination temperature of TiO_2, the higher the crystallinity, and the lower surface defect content, the lower the capability of TiO_2-to-molecule CT and the weaker SERS signals for the molecules on TiO_2. This illustrates that the intrinsic semiconductor surface states (surface defect) play an important role in the TiO_2-to-molecule CT process, both as electron traps and intermediate states for electron transfer to molecules. The plentiful surface states are favorable to a TiO_2-to-molecule CT process.

Moreover, the SERS effect for 4-MBA adsorbed on TiO_2 nanoparticles was also observed when using 457.9 nm radiation as exciting source, though weaker than those excited with 514.5 nm, since the 457.9 nm radiation was sufficient for excitation of the TiO_2-to-molecule CT (Figure 5c). The laser wavelength-dependent SERS for molecules adsorbed on TiO_2 nanoparticles will be detailed in a future report.

Conclusions

In this work, we observed SERS for the molecules adsorbed on TiO_2 nanoparticles for the first time. This is attributed to the contribution of the TiO_2-to-molecule CT mechanism related to the surface state energy level of TiO_2 nanoparticles. The CT process and the enhancement of Raman signals for the molecules on TiO_2 is largely dependent on the intrinsic nature of the adsorbed molecules and the surface property of semiconductor, both the stronger electron attracting ability of groups para- to the mercapto group bonded with TiO_2 surface and the plentiful surface states of TiO_2 nanoparticles are favorable to TiO_2-to-molecule CT and SERS for the molecules adsorbed on TiO_2.

Acknowledgment. The research was supported by National Natural Science Foundation (Grant Nots. 20473029, 20573041) of P. R. China, Program for Changjiang Scholars and Innovative Research Team in University (PCSIRT), Program for New Century Excellent Talents in University (NCET), Innovative Scholars of Jilin University (2004CX035), Fund for the Doctoral Program of Higher Education (20040183048), Scientific Research Foundation for the Returned Overseas Chinese Scholars initiated by State Education Ministry, Program of Introducing Talents of Discipline to Universities (B06009), Scientific and Technical Project of Jiamusi University (S2008-045).

References and Notes

(1) Nie, S. M.; Emory, S. R. *Science* **1997**, *275*, 1102–1106.
(2) Kneipp, K.; Wang, Y.; Kneipp, H.; Perelman, L. T.; Itzkan, I.; Dasari, R. R.; Feld, M. S. *Phys. Rev. Lett.* **1997**, *78*, 1667–1670.
(3) Xu, H.; Bjerneld, E. J.; Kall, M.; Borjesson, L. *Phys. Rev. Lett.* **1999**, *83*, 4357–4360.
(4) Tian, Z. Q.; Ren, B.; Wu, D. Y. *J. Phys. Chem. B* **2002**, *106*, 9463–9483.
(5) Ren, B.; Lin, X. F.; Yang, Z. L.; Liu, G. K.; Aroca, R. F.; Mao, B. W.; Tian, Z. Q. *J. Am. Chem. Soc.* **2003**, *125*, 9598–9599.
(6) Whitney, A. V.; Myers, B. D.; Van Duyne, R. P. *Nano Lett.* **2004**, *4*, 1507–1511.
(7) Haynes, C. L.; Van Duyne, R. P. *Nano Lett.* **2003**, *3*, 939–943.
(8) Tian, Z. Q.; Ren, B.; Li, J. F.; Yang, Z. L. *Chem. Commun.* **2007**, 3514–3534.
(9) Quagliano, L. G. *J. Am. Chem., Soc.* **2004**, *126*, 7393–7398.
(10) Hayashi, S.; Koh, R.; Ichiyama, Y.; Yamamoto, K. *Phys. Rev. Lett.* **1988**, *60*, 1085–1089.
(11) Wang, Y. F.; Hu, H. L.; Jing, S. Y.; Wang, Y. X.; Sun, Z. H.; Zhao, B.; Zhao, C.; Lombardi, J. R. *Anal. Sci.* **2007**, *23*, 787–791.
(12) Wang, B. Q.; Jing, L. Q.; Qu, Y. C.; Li, S. D.; Jiang, B. J.; Yang, L. B.; Xin, B. F.; Fu, H. G. *Appl. Surf. Sci.* **2006**, *252*, 2817–2825.
(13) Zhang, Q. H.; Gao, L.; Guo, J. K. *Appl. Catal., B* **2000**, *26*, 207–215.
(14) Choi, W.; Termin, A.; Hoffmann, M. R. *J. Phys. Chem.* **1994**, *98*, 13669–13679.
(15) Pérez León, C.; Kador, L.; Peng, B.; Thelakkat, M. *J. Phys. Chem. B* **2006**, *110*, 8723–8730.
(16) Sun, Z. H.; Zhao, B.; Lombardi, J. R. *Appl. Phys. Lett.* **2007**, *91*, 221106.
(17) Michota, A.; Bukowska, J. *J. Raman Spectrosc.* **2003**, *34*, 21–25.
(18) Lombardi, J. R.; Birke, R. L. *J. Phys. Chem. C* **2008**, *112*, 5605–5617.
(19) Otto, A.; Mrozek, I.; Grabhom, H.; Akemann, W. *J. Phys.: Condens. Matter* **1992**, *4*, 1143–1212.
(20) Moskovits, M. *Rev. Mod. Phys.* **1985**, *57*, 783–828.
(21) Metiu, H. *Prog. Surf. Sci.* **1984**, *17*, 153–320.
(22) Gersten, J. I.; Birke, R. L.; Lombardi, J. R. *Phys. Rev. Lett.* **1979**, *43*, 147–150.
(23) Osawa, M.; Matsuda, N.; Yoshii, K.; Uchida, I. *J. Phys. Chem.* **1994**, *98*, 12702–12707.
(24) Zhou, Q.; Li, X. W.; Fan, Q.; Zhang, X. X.; Zheng, J. W. *Angew. Chem., Int. Ed.* **2006**, *45*, 3970–3973.
(25) Kittel, C.; Zettl, A.; McEuen, P. *Introduction to Solid State Physics*; John Wiley and Sons: New York, 2004.
(26) Boschloo, G.; Fitzmaurice, D. *J. Phys. Chem. B* **1999**, *103*, 2228–2231.
(27) Jing, L. Q.; Qu, Y. C.; Wang, B. Q.; Li, S. D.; Jiang, B. J.; Yang, L. B.; Fu, W.; Fu, H. G.; Sun, J. Z. *Solar Energy Mater. Solar Cells* **2006**, *90*, 1773–1787.
(28) Jing, L. Q.; Xin, B. F.; Yuan, F. L.; Xue, L. P.; Wang, B. Q.; Fu, H. G. *J. Phys. Chem. B* **2006**, *110*, 17860–17865.
(29) Cao, Y. A.; Meng, Q. J.; Song, Q.; Shu, Y. C.; Zhao, J. Y.; Yao, J. H.; Bai, Y. B.; Xu, J. J. *Chem. J. Chin. Univ.* **2005**, *26*, 1677–1681.

JP8074145